International Journal of Scientific Research Updates

Journal homepage: https://orionjournals.com/ijsru/

ISSN: 2783-0160 (Online)

(RESEARCH ARTICLE)

Check for updates

Sorption of tartrazine dye from aqueous solution using activated carbon prepared from *Cocos nucifera* husk

Egah GO [1,*], Sha'Ato R [2], Itodo, AU [2] and Wuana RA [2]

[1] *Chemical Sciences Department, Faculty of Pure and Applied Sciences, Federal university Wukari, Taraba State, Nigeria.*
[2] *Chemistry Department, Faculty of Physical Sciences, Joseph Sarwuan Tarka University (Formerly Federal University of Agriculture) Makurdi Benue State, Nigeria.*

International Journal of Scientific Research Updates, 2023, 06(01), 093–106

Publication history: Received on 14 July 2023; revised on 31 August 2023; accepted on 02 September 2023

Article DOI: https://doi.org/10.53430/ijsru.2023.6.1.0061

Abstract

Sorption of Tartrazine dye from aqueous solution using activated carbon prepared from *Cocos nucifera* (coconut) husk was investigated in this work. The coconut shell was first carbonized at 700°C in a muffle furnace and activated with NaOH for one hour. The activated carbon (AC) was applied to remove tartrazine from aqueous solutions over a concentration range of 50-250 mg/L respectively. Adsorbent features were determined using X-ray fluorescence (XRF), Fourier transformed infrared spectroscopy (FTIR), Scanning electron micrograph (SEM) techniques. Based on this investigation, adsorption of Tartrazine dye is strongly affected by initial solution pH, initial solution concentrations, dosage, and time of contact which favours the removal. Except for temperature which was found to decrease with increase temperature for AC, while adsorption capacity of Tartrazine was found to decrease with increase in adsorbent dosage for AC. The optimum pH for adsorption Tartrazine removal was found to be 3. The experimental data of Tartrazine was found to fit the linearized Langmuir isotherm better than the Freundlich isotherm and D-R model indicating a monolayer adsorption. On effect of initial solution concentration, adsorption capacity of Tartrazine was found to increase with increase in concentration for AC. Kinetic data fitted more into pseudo second order model than first order and intra particle diffusion model, suggesting that chemisorption dominate the rate limiting step. The calculated thermodynamic parameters – Gibbs free energy, enthalpy change and entropy change indicated that adsorption of Tartrazine was endothermic and not spontaneous meaning the chemisorption dominates physisorption.

Keyword: Adsorption; Activated carbon; Coconut husk; Tartrazine dye

1. Introduction

In many industries like textiles, foods, paint, cosmetics, leather, paper-making and plastics, dyes are used as colorants [1]. Many dyes are made from carcinogens like benzidine which bio-accumulate, thus posing a serious threat [2]. Dye in water bodies reduced light penetration and decreased photosynthesis. High concentration of tartrazine causes permanent blindness, itching, liver and kidney damage, DNA mutation, dysfunction of central nervous system, mental disorders, asthma, decrease in RBC count (dyscrasia), eczema, thyroid cancer, hyperactivity and infertility [3, 4]. The removal of such dye from effluent before discharge into water bodies is therefore important. Various conventional technologies such as photo oxidation, ozonation, ultra-filtration, chemical precipitation, chlorination, reverse osmosis, biodegradation, chemical and physicochemical treatments have been used to remove tartrazine, but are far too expensive for many industries [5,6]. Therefore, a search for cheap raw materials for production adsorbents, which are more economical and effective in waste-water treatment, with minimal impact on human health. The adsorbents are used due to their large surface area, ion-exchange, adsorption, high versatility, easy manipulation and low costs in pollution remediation processes [7]. This research is aimed at preparation of activated carbon from coconut (*Cocos*

* Corresponding author: Egah GO

nucifera) husk, characterization of the adsorbent and assessment of the adsorbent for the removal of tartrazine dye, from aqueous solution using isotherm, kinetic and thermodynamic studies.

2. Materials and method

2.1. Materials

Method of activated carbon preparation was adopted from Ibrahim *et al.,* [8], with little modification. The *Cocos nucifera* (coconut) husk used as the raw material for the production of activated carbon were collected from New market Wukari, Taraba State Nigeria.

2.2. Preparation of Activated carbon

The coconut husk was washed several times using tap water and finally with distilled water, dried to constant weight at 120°C for 24 h in an oven to remove excess water content and then charred. The samples were crushed into smaller sizes for impregnation. A required mass of the crushed coconut husk sample was then soaked in water for 24 h and decanted. It was also soaked in dilute Tetra-oxosulphate (VI) acid (H_2SO_4) solution of 30% concentrations for 24 h and decanted. The samples were washed with distilled water to remove traces of acid from the sample. It was then dried using electric oven at temperature of 120°C for 12 h. The Impregnated sample was then carbonized in a muffle furnace at temperatures of 700 °C for 1 h and cooled. Activated carbon was produced by adding 0.1 M sodium hydroxide (NaOH) to the sample such that the solid to liquid ratio is 1:10 in g/cm^3. The mixtures were left overnight at room temperature in a conical flask. After, 24 h the supernatant liquid was decanted in a filter paper followed by successive washing and decanting using distilled water until the pH Value is approximately 7 (neutral stage). The sample was then dried in an oven at temperature of 110 °C for 2 h. The carbonized coconut shell produced was allowed to cool and weighed. The dry biomass was crushed and sieved into particle size 0.045 mm - 0.150 mm.

2.3. Scanning Electron Micrographs (SEM) Analysis

Scanning electron microscopy (SEM) was used to determine the surface structure and shape of an adsorbent or catalyst [9]. The SEM imaging was carried out at multidisciplinary central laboratory, University of Ibadan, Oyo State. Scanning electron microscope (SEM - JEOL, JSM 7600 F) was used to determine the surface texture and porosity of the adsorbent and catalyst. A thin layer of platinum was sputter-coated on the adsorbent for charge dissipation during SEM imaging. The sputter coater (Eiko IB-5 Sputter Coater) was operated in an argon atmosphere using a current of 6 mA for 3 min. The coated samples were then transferred to the SEM specimen chamber and observed at an accelerating voltage of 5 kV, eight spot size, four aperture and 15 mm working distance [10].

2.4. Fourier Transformed Infra-red (FTIR) Analysis

The FT-IR was carried out at multidisciplinary Central Laboratory, University of Ibadan, Oyo State. This method of analysis was conducted to determine the existence of the surface functional groups of the adsorbent. The Fourier transform infrared (FTIR) spectra were collected in the range of 350-4400 cm^{-1} using the KBr disk method [10].

2.5. X-ray Fluorescence (XRF) Analysis

The XRF analysis was carried out at Engineering materials development institute, Akure, Ondo State. Sky-ray Instrument (EDX3600B X-ray fluorescence) was used. This method of analysis was used to determine the chemical composition of the adsorbent. The samples were pulverised to fine homogeneous size and then pelletized before analysis.

2.6. Preparation of Tartrazine Stock Solution

Method of adsobate preparation was adopted from Makeswari *et al.,* [11]. The stock solution of 500 mg/L was prepared by dissolving 0.5 g of analytical grade tartrazine dye in 1 liter volumetric flask and made up to the mark with deionized water. Several standard concentrations of tartrazine (20, 40, 60, 80, 100 mg/L) were prepared from the stock solution by serial dilution using Equation (1):

$$C_1V_1 = C_2V_2 \qquad (1)$$

where: C_1 = concentration of stock solution.
C_2= the desired concentration to be prepared.
V_1= volume of stock solution to be taken

V_2= volume factor to be diluted with

2.7. Batch Adsorption Experiments

Batch experiments were carried out according to methods adopted by Sha'Ato *et al.,* [12]. In the batch experiment, 0.5 g of the adsorbent was contacted with 50 mL of 50 mg/L adsorbate solution in a conical flask (250 mL) in capacity, and stirred for (60 minutes) constant contact time by mechanical shaker at (200 rpm) at room temperature until equilibrium is achieved. At the end of the contact time required, the solutions were centrifuged and filtered using whatman No. 1 filtered paper, and the filtrate analyzed for residual tartrazine concentration, using UV-visible spectrophotometer (Shimadzu, UV-1700 spectrophotometer) at a maximum wavelength of 426 nm [13]. Batch adsorption experiments were performed by varying the pH, adsorbent dosage, concentration, contact time and temperature. In each experiment, the studied parameter was varied while others were kept constant. The experiments were repeated in triplicate to minimize errors. In the batch adsorption experiment, the amount Qe (mg/g), of tartrazine was expressed as equation 2-3 [13].

$$Q_{e\,(mg/g)} = \frac{(C_o - C_e)}{M_a} v \qquad (2)$$

$$\% \text{ Removal} = \left(\frac{C_o - C_e}{C_o}\right) \times 100 \qquad (3)$$

where C_0 (mgL^{-1}) is the concentration of the tartrazine solution at starting time (t = 0), Ce (mgL^{-1}) is the concentration of the tartazine solution at equilibrium time, V (L) is the volume of the solution treated used in litre (L) and M_a (g) is the mass of the adsorbent.

2.7.1. Adsorption isotherm

In this study, Langmuir, Freundlich and D-R adsorption isotherms were used to describe the experimental data. The Langmuir adsorption isotherm equation is based on assumption that the maximum adsorption occurred due to a saturated mono-layer of adsorbate molecules on the adsorbent surface [14]. According to Asiagwu *et al.,* [15], the Langmuir adsorption isotherm is expressed as Equation (4):

$$q_e = Q_m \cdot \frac{bc_e}{1 + bC_e} \qquad (4)$$

The linear Langmuir adsorption isotherm is expressed as Equation (5):

$$\frac{1}{Q_e} = \frac{1}{Q_m} + \frac{1}{C_e} \times \frac{1}{bQ_m} \qquad (5)$$

where Q_m (mg/g**)** is the monolayer sorption capacity at equilibrium for the Adsorbate-Adsorbent which is the total number of binding sites that are available for sorption, C_e is the equilibrium concentration of the solute in the bulk solution (mg/L), Q_e (mg/g) is the amount of solute sorbed per unit mass of the adsorbent at equilibrium which is the number of binding sites that are occupied by the sorbate at equilibrium concentration and b (L/mg) is the Langmuir constant for the Adsorbate-Adsorbent. The higher the magnitude of b, the higher the heat of sorption and the stronger the bond formed [16]. A linear plot of $1/Q_e$ versus $1/C_e$ gives a straight line graph, with the slope and the intercept of $1/Q_m$ and $1/bQ_m$, respectively. The characteristics of the langmuir isotherm was determined by the dimensionless constant called separation factor, R_L expressed as Equation (6):

$$R_L = \frac{1}{(1 + bC_0)} \qquad (6)$$

Where b (L/mg) is the Langmuir constant for adsorbate-adsorbent and C_0 (mg/L) the initial adsorbate concentration. R_L indicates the nature of adsorption process shown as: $R_L > 1$, is unfavourable, $R_L = 1$ is linear, R_L between 0 - 1 is favourable and $R_L = 0$ is irreversible [12].

The Freundlich isotherm is based on multilayer adsorption on the heterogeneous surface of the adsorbent containing an unequal amount of energies [17]. The general form of Freundlich adsorption isotherm as adopted by Al-Ghouti and Da'ana, [14], is given as Equation (7):

$$q_e = \mathrm{K_f} C_e^{\frac{1}{n}} \qquad (7)$$

The linear equation of Freundlich isotherm as adopted by Sha'Ato *et al.,* [12], is given as Equation (8):

$$logQ_e = \frac{1}{n} logc_e + logK_f \quad (8)$$

where Q_e (mg/g) is the amount of adsorbate sorbed per unit mass of the adsorbent and C_e (mg/L) is the equilibrium concentration of the adsorbate. K_f is the Freundlich constants related to the adsorption capacity and 1/n is a function of the strength of adsorption, which varies with the heterogeneity of the material [18]. 1/n is a function of the strength of adsorption, which varies with the heterogeneity of the material. A linear plot of log Q_e versus log C_e gives the slope of n and intercept K_f. If the value of n lies in the range of 1 - 10, they are classified as favourable adsorption according to Freundlich as reported by Sha'Ato *et al.,* [12].

Dubinin-Radushkevich (D-R) helps to determine the adsorption mechanism. It distinguished between the chemical adsorption and physical adsorption. D-R Equation as adopted by Al-Ghouti and Da'ana, [14], is given as Equation (9):

$$q_e = q_m{}^{-K\varepsilon^2} \quad (9)$$

The linear form is given as Equation (10)

$$Inq_e = lnq_m - K\varepsilon^2 \quad (10)$$

Where, Q_e = amount of adsorbate adsorbed per unit weight of adsorbent at equilibrium (mgg^{-1}), Q_m = Maximum adsorption capacity of adsorbent (mgg^{-1}), K = constant related to adsorption energy, ε = polanyi potential (kJ^2mol^{-2}). ε can be acquired from equation (11)

$$\varepsilon = RTln(1 + \frac{1}{C_e}) \quad (11)$$

where, R is the universal gas constant, T is the standard temperature in (K), Ce is the concentration of adsorbate at equilibrium in solution after adsorption (mgl^{-1}). The experimental data can be evaluated by plotting lnQe against ε^2. The values of Q_m and K are estimated from the intercept and slope respectively. The mean adsorption energy is calculated with the Equation (12):

$$\varepsilon = \frac{1}{\sqrt{2K}} \quad (12)$$

Values of ε less than 8 $kJmol^{-1}$ showed a physical adsorption, while values between 8-16 $kJmol^{-1}$ showed a chemical adsorption [14].

2.8. Adsorption Kinetics

Chemical kinetics deals with the experimental conditions influencing the rate of a chemical reaction. Herein, three kinetic models including the pseudo-first-order, pseudo-second-order and intra-particle diffusion model were used to analyze the experimental data of the sorption process. The Pseudo first order model is used for adsorbate - adsorbent in liquid- solid phase adsorption experiment. The Lagergren rate Equation of pseudo-first order is given in Equation (13) [19]:

$$\log(Q_e - Q_t) = logQ_e - \frac{K_1}{2.303} t \quad (13)$$

where Q_t is the amount of adsorbate adsorbed per unit of adsorbent (mg/g) at contact time t (min), Q_e is the amount of adsorbate adsorbed per unit mass of the adsorbent in (mg/g), k_1 is the pseudo first order rate constant (L/min). A linear plot of log (Q_e-Q_t) versus t gives k_1 as the r ate constant, $-\frac{K_1}{2.303}$ as the slope and log Q_e as the intercept [19].

The Blanchard pseudo-second order model rate equation as adopted by Rajesh *et al.,* [20], is also presented in Equation (14):

$$\frac{t}{Q_1} = \frac{1}{K_2 {Q_e}^2} + \frac{1}{Q_e} t \quad (14)$$

where K_2 is the pseudo-second order rate constant (g.mg^{-1}.min$^{-1)}$ and the initial adsorption rate, h (mg/g.min) = $K_2Q_e^2$. A linear plot of $\frac{t}{Q_t}$ versus t gives us K_2 the second- order rate constant, $\frac{1}{Q_e}$ as the slope and $\frac{1}{K_2 Q_{e^2}}$ as the intercept [21].

The Intra-particle diffusion model is used to identify the diffusion mechanism during the adsorption process, so the experimental data were tested by the intra-particle diffusion model, which can be expressed as equation (15):

$$Qt = kt^{0.5} + C \quad (15)$$

Where qt (mg/g) is the amount of adsorbate adsorbed at time t (min), k (mg/g min$^{1/2}$) is the intra-particle diffusion rate constant and C is the intercept [22, 19].

2.9. Thermodynamics Studies

Van't Hoff equation is used to connect chemical equilibrium constant and temperature by thermodynamics relation of Gibbs-Helmholtz free energy equation. The spontaneity of the adsorption process is usually described by changes in the standard Gibb's free energy (ΔG°) in (kJmol^{-1}), standard enthalpy change (ΔH^0) in (kJmol^{-1}) and the standard entropy change (ΔS^0) in (JK^{-1}mol^{-1}). These helps provide a better understanding of the adsorption process [23]. The linearize form of Van't Hoff equation is given as Equation (16):

$$\log(\frac{q_e}{C_e}) = \frac{\Delta S^\circ}{2.303R} - (\frac{\Delta H^\circ}{2.303R})\frac{1}{T} \quad (16)$$

where Q_e/C_e is the adsorption affinity, R is the universal gas constant (8.314 Jmol^{-1}K^{-1}), T is the temperature in (K). The thermodynamic parameters were calculated from the plot of $\log(qe/C_e)$ versus $1/T$, which gave a straight line graph, where –(ΔH^0/2.303R) is the slope and (ΔS^0/2.303R) is the intercept. The free Gibbs energy is calculated using Equation (17):

$$\Delta G^\circ = \Delta H^\circ - T\Delta S^\circ \quad (17)$$

where T is the standard temperature (298 K).

If ΔG˚ is a negative value at a given temperature, the reaction occurs spontaneously. Adsorption is considered as exothermic reaction when ΔH˚ is a negative value, while it is an endothermic reaction if ΔH˚ is a positive value. The affinity of the adsorbent towards the adsorbate is reflected by the positive ΔS˚ value, indicating an increase in randomness [14]. It is suggested by the thermodynamic relation between ΔG˚, ΔH˚ and ΔS˚ that either (i) ΔH˚ or ΔS˚ are negative and ΔH˚ > TΔS˚, (ii) ΔH˚ or ΔS˚ are positive and TΔS˚ > ΔH˚, (iii) ΔH˚ is negative and ΔS˚ is positive [24,14].

3. Results and discussion

3.1. FTIR analysis of the adsorbent

Table 1 FT-IR Analysis of Activated Carbon

Group Freq (cm^{-1})	Functional groups	AC - Observed Frequency (cm^{-1})	Assignment
4000-3000	Alcohol/Phenol	3480.00	-OH stretch
3000-2000	Alcohol/Phenol	2000.00	-OH stretch
1680–1620	Alkenes	1640.31	O-H Bend vibration
1035-1080	Alcohol	1071.00	Si-O stretch
900 – 670	Aromatic	803.21	Si-O stretching vibration
550-200	Alkyl halides	461.00	Si-O-Si deformation

The FT-IR analysis of activate carbon (AC), in Table 1 and Figure 1a, showed bands at 3480.00 cm^{-1}, 2000.00 cm^{-1}, within the frequency range of (2000-4000 cm^{-1}) representing the stretching vibrations of O-H group. The band at 1640.31cm^{-1} is attributed to Si-O stretch from Silica [25]. The band at 1071.00 cm^{-1} and 803.21 cm^{-1} are attributed to O-H bend and

Si-O-Si deformation. Similar results were reported by Gupta and Nayak, [26], studies on cadmium removal and recovery from aqueous solution by novel adsorbent prepared from orange peel and Fe_2O_3 nanoparticles.

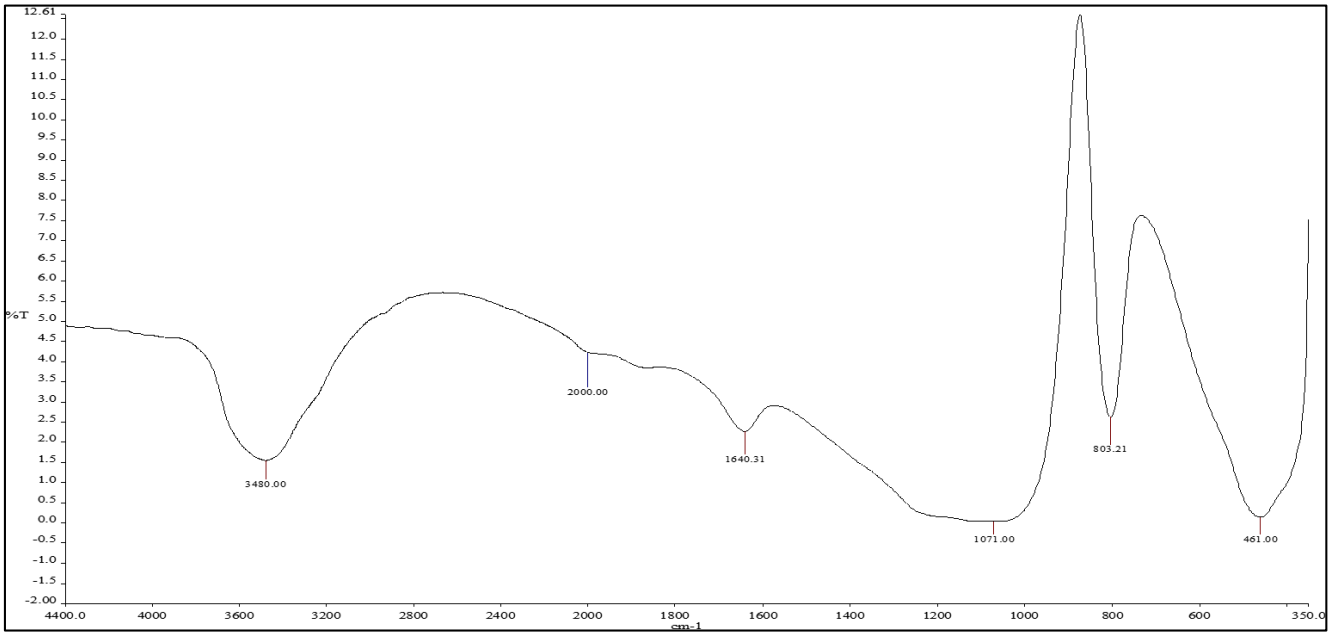

Figure 1a FTIR Spectrum of Activated Carbon prepared from *Cocos Nucifera* Shell for Adsorption

3.2. XRF characterization of adsorbent

Table 2 X- Ray Fluorescence Characterization of the Activated Carbon (AC)

Oxide	**AC (wt %)**
Al_2O_3	2.3598
SiO_2	0.7763
P_2O_5	0.5743
SO_3	14.2273
K_2O	1.3813
CaO	0.4717
FeO	0.6411
CuO	0.3966
ZnO	0.3579
WO_3	0.7826
SnO_2	2.7525
Sb_2O_5	2.2297

The chemical composition of the sorbent activated carbon (AC) was determined using X-Ray Florescence instrument (XRF) as shown in Table 2. This was performed using a voltage of 40 kv and 350 µA current. The results shows that AC is composed of Al_2O_3 (2.3598 %), SiO_2 (0.7763 %), P_2O_5 (0.5743%), SO_3 (14.2273 %), K_2O (1.3813 %), CaO (0.4717 %), FeO (0.6411 %), CuO (0.3966 %), ZnO (0.3579 %), WO_3 (0.7826 %), SnO_2 (2.7525 %) and Sb_2O_5 (2.2297 %). It is thus expected that Tartrazine in solution could be removed mainly by SiO_3 and Al_2O_3 [27]. Similar observations were reported by Dawodu *et al.* [27], studies on isotherm modeling on the equilibrium sorption of Cadmium (II) from Solution by Agbani Clay.

3.3. Scanning Electron Microscopy of Adsorbents

SEM results show the surface morphology feature of the adsorbent, which is an indication that an important interaction can occur between the adsorbate and adsorbent - granule interface in the experimental conditions [13]. Figure 1b shows the micrograph of AC. From the result in Figure 1b, it is observed that the AC adsorbent showed a rough surface, with some cavity. According to Gupta and Nayak, [26], adsorbents with fine porous structure are good for adsorption process.

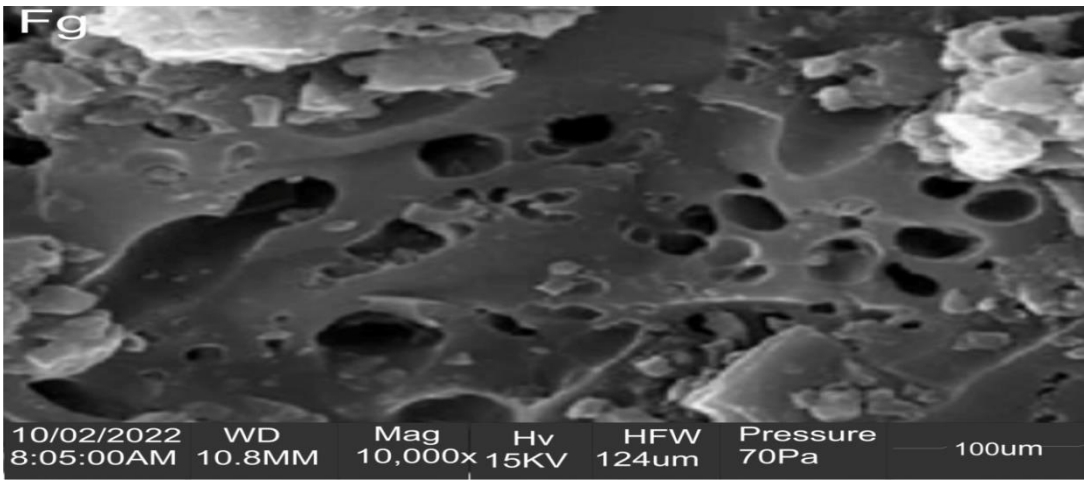

Figure 1b Scanning Electron Micrograph (SEM) AC

3.4. Effect of Initial Solution pH on Adsorption of Tartrazine

Figure 2, showed the effect of pH on adsorption of Tartrazine. Results showed the highest percentage removal of tartrazine was observed for AC at pH 3, indicating it optimum pH. This may be due to increase in electrostatic attraction between the adsorbate and adsorbent. Tartrazine dissociates into negatively charge species, which could be easily adsorbed on positively charged surfaces of adsorbents in electrostatic attraction between the adsorbate and adsorbent [13].

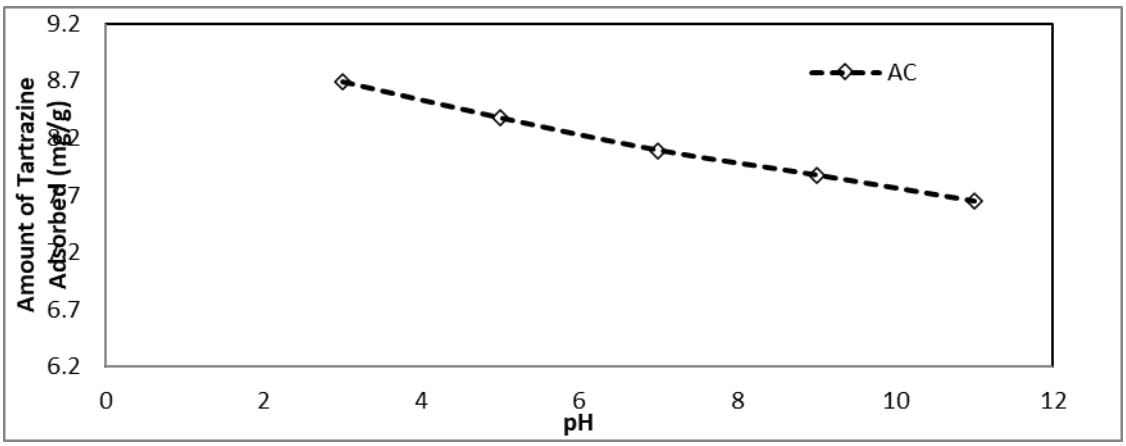

Figure 2 Effect of Initial Solution pH on Aqueous Phase Adsoprtion of Tartrazine by Activated Carbon

3.5. Effect of Adsorbent Dosage on Tartrazine

From the results in Figure 3, it was observed that as the dosage increased from 0.5 g - 2.5 g for AC, adsorption capacity decreased with increase in adsorbent dosage. The decreasing trend in the amount of tartrazine removed may be attributed to overlapping of the active site which resulted in decrease in adsorption capacity [3]. Similar trend was reported by Sartape *et al.,* [3], study on the removal of malachite green dye from aqueous solution with adsorption technique using *Limonia acidissima* (wood apple) shell as low cost adsorbent.

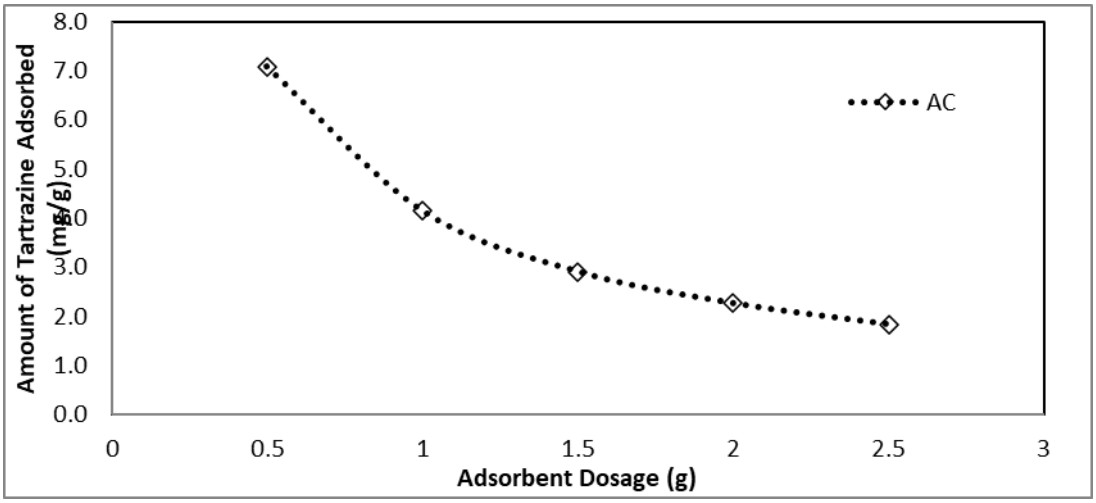

Figure 3 Effect of Adsorbent Dosage on Aqueous Phase Dissipation of Tartrazine via Adsorption by Activated Carbon

3.6. Effect of Initial Concentration on Adsorption of Tartrazine

Figure 4, showed the plot for equilibrium concentration of tartrazine. From the result, it was observed as the initial concentration of tartrazine dye increases from 50 – 250 mg/L that the amount adsorbed by AC increases from 3.1242 – 13.7884 mg/g. Similar observation for Cu (II) ions uptake on different sorbents have been reported by Bayat, [28].

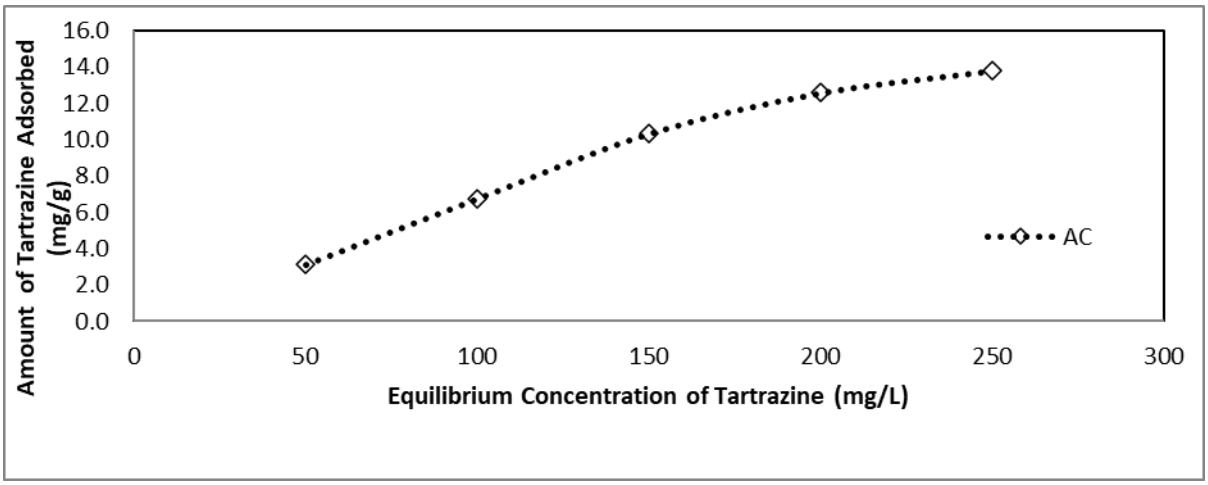

Figure 4 Effect of the Initial Concentration on Aqueous Phase Dissipation of Tartrazine via Adsorption by Activated Carbon

3.7. Adsorption Kinetics

3.7.1. Rate curve for Adsorption of Tartrazine

The rate curve for tartrazine is as shown in Figures 5. From the result in Figures 5, it was observed that adsorption capacity increased at all times from 10 minutes until equilibrium was attained at 60 minutes. Adsorption rate appeared to be very fast from the beginning, which could be explained due to the high number of active sights present at the starting point [29]. As the process continues, the adsorption sites became saturated. The uptake rate was controlled by the rate at which the adsorbate is transported from the exterior to the interior sites of the adsorbent particles, so the adsorption became much slower until saturation was attained at 60 minutes [30]. The highest adsorption capacity of 9.0027 mg/g was observed for Tartrazine at 60 minutes.

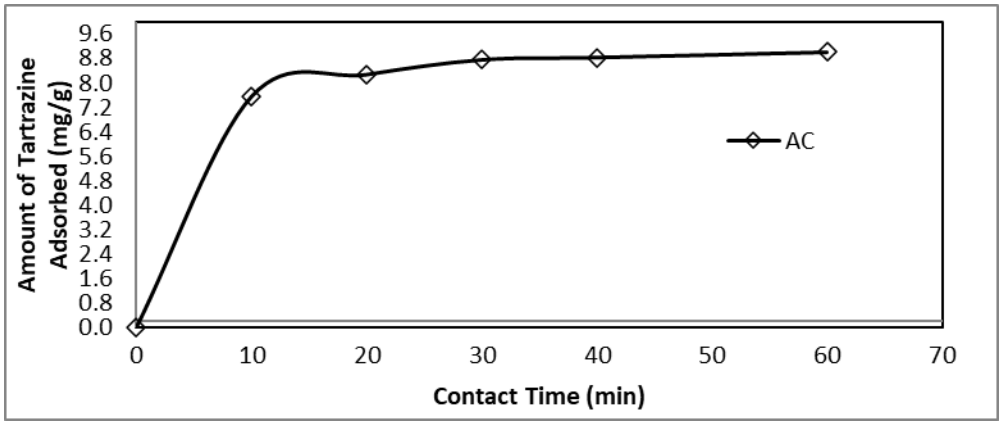

Figure 5 Rate Curves on Aqueous Phase Dissipation of Tartrazine via Adsorption by Activated Carbon

3.8. Adsorption kinetic model

Data that were obtained from the effect of contact time on adsorption Tartrazine were fitted into the kinetic model. The result from the kinetic parameters in Table 3 and Figures 6 showed that the adsorption of Tartrazine on AC could be described by first order, second order and intra particle diffusion model. Based on correlation coefficient R^2, it was observed that the Blanchard pseudo-second order gave better fittings closer to unity for Tartrazine with R^2 value (0.9999) than the values 0.0491 and 0.8779 for pseudo-first order and intra particle diffusion model respectively. The high value of regression coefficient for the second - order shows that the pseudo second order equation best describes the entire adsorption process [31]. This implies that adsorption on AC occurs through a chemical process involving the valence forces of exchanged electrons indicating chemisorption as predominant rate-controlling step for the system [31].

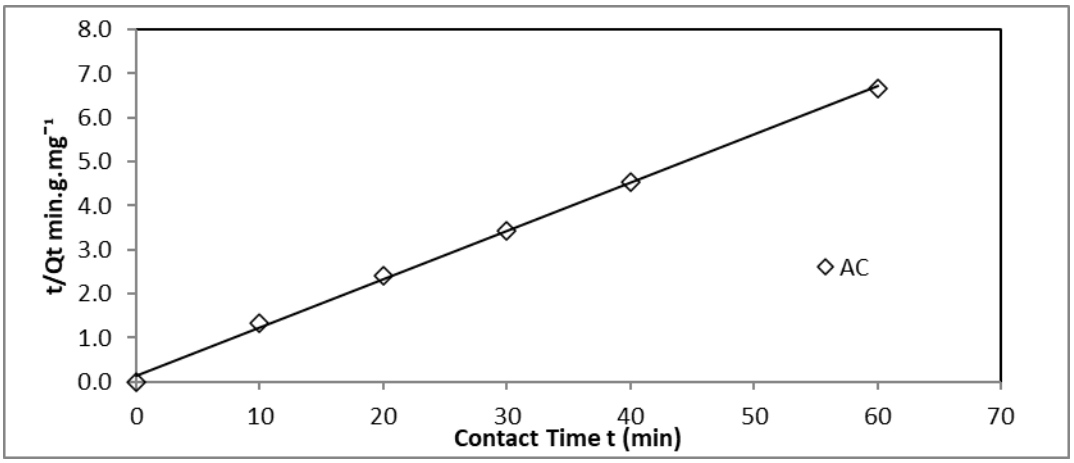

Figures 6 Blanchard Pseudo-Second Order Kinetic Plots for Dissipation of Tartrazine via Adsorption by Activated Carbon

Table 3 Kinetic Parameter for Adsorption Lagergren First Order, Blanchard Second Order and Intra Particle Diffusion Kinetic Model for Tartrazine.

Adsorbate	**Model**	**Adsorbents**
Tartrazine	First order	AC
	K_1 ($Lmin^{-1}$)	0.0106
	Qe (mg/g)	0.7542
	R^2	0.0491
	Second order	

	K_2 (g.mg^{-1}min^{-1})	0.04396
	Qe (mg/g)	9.3720
	R^2	0.9999
	h (gmg^{-1}min^{-1})	3.8610
	Intra Particle Diffusion	
	K_{diff} (mg/g.min$^{1/2}$)	0.3130
	C	6.7817
	R^2	0.8779

3.9. Adsorption Isotherm Models

Results on Table 4 and Figure 7 shows the plots obtained for the Langmuir, Freundlich and Dubunin-Radushkevich D-R adsorption isotherm models for the pollutants; tartrazine dye. On the assumption that adsorption occurs at homogeneous sites in monolayer and heterogeneous surface in multilayer adsorption, Langmuir and Freundlich models were used respectively [32]. For the Langmuir results in Table 4, the maximum adsorption capacity, Q_m for AC was found to be (333.333) mg/g, which represents, the total adsorbate – adsorbent binding capacity. The separation factor (R_L); a useful dimensionless parameter which described the suitability of AC adsorbent and its affinity towards tartrazine dye was determined. Four probabilities exist for the value of R_L: $R_L > 1$, $R_L = 1$, $0 < R_L < 1$, and $R_L = 0$, indicating unfavorable, linear, suitable, and irreversible degrees, respectively. From results on Table 4, the calculated Langmuir separation factor R_L, for tartrazine dye was found to be 0.9744, indicating the suitability of the adsorption process using porous AC adsorbent [33]. From the results on correlation coefficients R^2 on adsorption of tartrazine dye as described by Langmuir and Freundlich isotherms in Table 4. The Langmuir gave higher R^2 values of (0.9490) for Tartrazine dye as compared with Freundlich with value (0.8948), indicating that the experimental data best obey the Langmuir isotherm, than the Freundlich for tartrazine. This implied that the Langmuir model best describe the experimental data and the uptake of tartrazine analytes and occurred on a homogenous surface by monolayer adsorption and there is a uniform distribution of the heat of adsorption over AC surface [33]. From the Freundlich model results in Table 4, tartrazine has a K_F value of 0.3439 mg/g. The results also showed the value of $1/n_F$ to be 0.8239, which is less than unity indicating favourable adsorption onto AC [34]. The nF value was found to be 1.2137 for tartrazine dye. For values of nF = 1, the adsorption is linear; nF < 1, indicate a chemical adsorption process and nF > 1, indicates a favourable physical adsorption process [35].

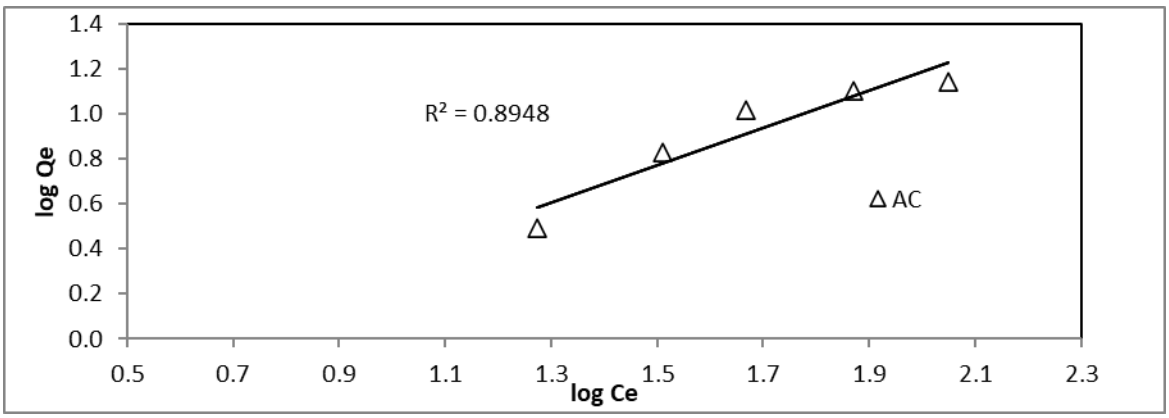

Figure 7 Freundlich Isotherm for Dissipation of Tartrazine Dye via Adsorption by Activated Carbon

This implies that the adsorption process is a physical process. These criteria is in agreement with Bousba and Meniai, [36], studies on the Adsorption of 2-Chlorophenol onto Sewage Sludge based Adsorbent. For the Dubunin-Radushkevich D-R isotherm models for adsorption, Equilibrium data for the adsorption of tartrazine from aqueous phase were fitted in the linearized forms of the Dubunin-Radushkevich D-R models. Their parameters are presented in Table 4. The Q_m, (mg/g) value for Tartrazine was found to be (13.3644,) mg/g. The high binding site of AC, may be attributed to it

porosity and large surface area [15,14]. The polanyi potential (ε) (kJ^2mol^{-1}) for the D-R, was found to be greater than 8 $kJmol^{-1}$ indicating that the process proceeds chemically [17]. This result is different from that of Freundlich isotherm.

Table 4 Isotherm Parameters for Tartrazine Dye Adsorption on Activated Carbon

Adsorbate	**Model**	**Adsorbent**
Tartrazine	Langmuir	AC
	Q_m(mg/g)	333.3333
	b (L/mg)	0.0005
	R^2	0.9490
	R_L	0.9744
	Freundlich	
	1/n	0.8239
	n_F	1.2137
	R^2	0.8948
	K_F((mg/g) L/mg)1/n)	0.3439
	D-R	
	Q_m, (mg/g)	13.3644
	K (mol^2/kJ^2)	9E-5
	ε (kJ/mol)	76.1035
	R^2	0.9749

3.10. Thermodynamic Parameter for Adsorption of Tartrazine

Results in Table 5, showed the calculated values of thermodynamic parameters. From table 5, the positive value of ΔH^0 (9.741 $kJmol^{-1}$), indicates that endothermic reaction of adsorption process dominates, of which chemisorption dominates physisorption [12]. Hence high temperature does not favour the adsorption phenomenon. Similar observation and explanation have been given by Sartape *et al.,* [3], studies on the removal of malachite green dye from aqueous solution with adsorption technique using *Limonia acidissima* (wood apple) shell as low cost adsorbent. The negative value of ΔS^0 (-40.672 J/molK) for AC, is attributed to high degree of disorderliness at the solid- liquid interface during adsorption reaction processes [37]. While the positive value of Gibbs free energy ΔG^0 for tartrazine of (23.081 kJ/mol) is an indication that the reaction is not spontaneous in nature [38]. According to Dula *et al.,* [39], ΔG^0 values from (80- 400 $kJmol^{-1}$) indicate that chemisorption dominates physisorption.

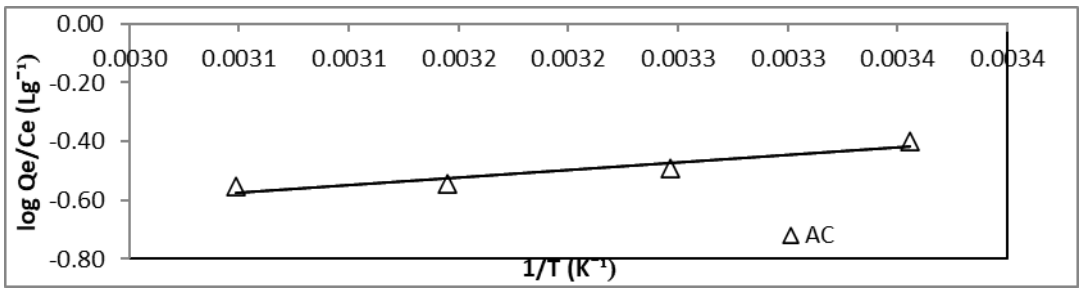

Figure 8 Van't Holf Plots for Dissipation of Tartrazine via Adsorption by Activated Carbon

Table 5 Thermodynamic Parameters of Adsorption of Tartrazine

Adsorbate	Adsorbents	ΔH(kJ/mol.1000)	ΔS(J/molK)	R^2	ΔG(kJ/mol.1000)
Tartrazine	AC	9.741	-40.672	0.909	23.081

4. Conclusion

From this study it could be concluded that adsorption of tartrazine dye onto Activated Carbon AC was affected by initial pH, adsorbent dosage, initial solution concentrations, temperature and contact time. From the investigation, adsorption capacity of tartrazine decreased with increase in adsorbent dosage for AC. The pH 3 was found to be the optimum pH for adsorption of tartrazine dye. For the effect of initial solution concentration and temperature, it was found that adsorption capacity of AC increased with increased in concentration and temperature for tartrazine dye. The adsorption isotherm and kinetics of the process favoured Langmuir isotherm and pseudo-second order models respectively, suggesting a monolayer adsorption. From the results it is found that chemisorption dominates physisorption. The activated carbon displayed a remarkable efficiency and effectiveness in the practical removal of tartrazine and can thus be recommended to dye industries to encourage the use agricultural waste to save cost and maximize profit.

Compliance with ethical standards

Acknowledgement

The authors appreciate Mr Edmond Luke and management of Chemistry laboratory Federal university wukari, Taraba State, Nigeria for their assistance.

Disclosure of conflict of interest

The authors declare that there are no conflicts of interest regarding the publication of this paper.

References

[1] Huang, Z., Li, Y., Chen, W., Shi, J., Zhang, N., Wang X., Li, Z., Gao, L and Zhang, Y. (2017). Modified bentonite adsorption of organic pollutants of dye wastewater, Materials Chemistry and Physics doi: 10.1016/j.matchemphys.2017.09.028

[2] Ratna and Padhi, B.S. (2012). ''Pollution due to synthetic dyes toxicity & carcinogenicity studies and remediation'' International Journal of Environmental Sciences, 3(3).

[3] Sartape A.S., Mandhare A.M., Jadhav V.V., Raut P.D., Anuse M.A and Kolekar S.S, (2017). Removal of malachite green dye from aqueous solution with adsorption technique using Limonia acidissima (wood apple) shell as low cost adsorbent, Arabian Journal of Chemistry, 10: S3229 –S3238

[4] Prajapati, A.K and Mondal, M.K. (2020). Comprehensive kinetic and mass transfer modeling for methylene blue dye adsorption onto CuO nanoparticles loaded on nanoporous activated carbon prepared from waste coconut shell, Journal of Molecular Liquids, https://doi.org/10.1016/j.molliq.2020.112949

[5] Berez A., Ayari F., Abidi N., SchaFer G and Trabelsi-Ayadi, M (2014). Adsorption-desorption processes of azo dye on natural bentonite: batch experiments and modeling, Clay Minerals, 49: 747–763

[6] Srivastav, M., Gupta, M., Agrahari, S. K and Detwal, P. (2019). Removal of Refractory Organic Compounds from Wastewater by Various Advanced Oxidation Process - A Review, Current Environmental Engineering, 6, 8-16

[7] De Gisi, S., Lofrano G., Grassi M and Notarnicola M (2016). Characteristics and adsorption capacities of low-cost sorbents for wastewater treatment: A review, Sustainable Materials and Technologies 9: 10 – 40

[8] Ibrahim, M.D., Shuaibu R., Abdulsalam S and Giwa S.O. (2016). Remediation of Escravous Crude Oil Contaminated Soil Using Activated Carbon from Coconut Shell, Journal of Bioremediation & Biodegradation, Volume 7, Issue 5

[9] Naswir, M., Arita, S., Marsi and Salni. (2013). Characterization of Bentonite by XRD and SEM-EDS and Use to Increase PH and Color Removal, Fe and Organic Substances in Peat Water. Journal of Clean Energy Technologies, 1(4): 313-317.

[10] Johari, K., Saman, N., Song, S.T., Heng, J.Y.Y. and Mat, H. (2014). Study of Hg(II) Removal from Aqueous Solution Using Lignocellulosic Coconut Fiber Biosorbents: Equilibrium and Kinetic Evaluation Journal, 44: 1198-1220.

[11] Makeswari. M., Santhi. T and Ezhilarasi M. R. (2016). "Adsorption of methylene blue dye by citric acid modified leaves of Ricinus communis from aqueous solutions", Journal of Chemical and Pharmaceutical Research, , 8(7):452-462

[12] Sha'Ato, R., Egah, G.O. and Itodo, A.U. (2018). Aqueous phase abatement of phenol and cadmium using Hydroxyiron (III) calcined with bentonite. Fuw Trends in Science and Technology Journal, 3(1): 1 – 10.

[13] Egah, G. O., Hikon, B. N., Ngantem, G. S, Yerima, E. A., Omovo, M., Ogah E and Aminu, F. A. (2019). Synergistic Study of Hydroxyiron (III) and Kaolinite Composite for the Adsorptive Removal of Phenol and Cadmium. International Journal of Environmental Chemistry. 3(1): 30-42. doi: 10.11648/j.ijec.20190301.15

[14] Al-Ghouti M. A and Da'ana D.A. (2020). Guidelines for the use and interpretation of adsorption isotherm models: A review, Journal of Hazardous Materials, 393: 122383

[15] Asiagwu, A.K., Emoyan O.O and Ojebah C.K (2018). Removal of Tartrazine Yellow Dye From Aqueous Solution using Groundnut Shell as Biomass: Kinetic Approach, International Journal of Engineering Research & Technology, 7(5): 404 – 411

[16] Chen X. (2015). Modeling of Experimental Adsorption Isotherm Data. Open access Information journal, 6:14-22

[17] Okeola F. O., Odebunmi E.O., Ameen O. M., Amoloye M. A., Lawal A. A and Abdulmummeen A. G (2017). Equilibrium Kinetics and Thermodynamic Studies of the Adsorption of Tartrazine and Sunset Yellow, Arid Zone Journal of Engineering, Technology and Environment, 13(2):268-280

[18] Bansal, R.C. and Goyal, M. (2005). Activated carbon adsorption. Journal water resource and protection, 6(9): 145-196

[19] Dada, A. O, Adekola F. A and Odebunmi E. O. (2017). "Kinetics, mechanism, isotherm and thermodynamic studies of liquid-phase adsorption of Pb2+ onto wood activated carbon supported zerovalent iron (WAC-ZVI) nanocomposite", Cogent Chemistry, (3), 1351653

[20] Rajesh, Y., Pujari, M and Uppaluri, R. (2014). Equilibrium and Kinetic Studies of Ni (II) Adsorption using Pineapple and Bamboo Stem Based Adsorbents, Separation Science and Technology, 49: 533–544

[21] Essomba, S. J., Ndi Nsami, J., Belibi Belibi, B. P., Tagne, M. G and Ketcha Mbadcam, J (2014). Adsorption of Cadmium(II) Ions from Aqueous Solution onto Kaolinite and Metakaolinite. Journal, Pure and Applied Chemical Sciences, 2(1): 11 – 30

[22] Balarak D and Mahdavi Y (2016). Experimental and Kinetic Studies on Acid Red 88 Dye (AR88) Adsorption by Azolla filiculoides, Biochemistry & Physiology: 5:1

[23] Dawodu, M.O and Akpomie K.G. (2016). Evaluating the potential of a Nigerian soil as an adsorbent for tartrazine dye: Isotherm, kinetic and thermodynamic studies, Alexandria Engineering Journal, 55: 3211–3218

[24] Ashraf M.W., Abulibdeh N and Salam A. (2019).Adsorption Studies of Textile Dye (Chrysoidine) from Aqueous Solutions Using Activated Sawdust, International Journal of Chemical Engineering, 9728156: 1-8

[25] El-Dars, E. S. M. F., Ibrahim, M. H., Farag, B. A. H., Abdelwahhab, Z. M and Shalabi H. E. M. (2016). Preparation, Characterization of Bentonite Carbon Composite And Design Application In Adsorption of Bromothymol Blue Dye. Journal of Multidisciplinary Engineering Science and Technology, 3(1): 3758-3765.

[26] Gupta, K.V and Nayak, A (2011). Cadmium removal and recovery from aqueous solutions by novel adsorbents prepared from orange peel and Fe2O3 nanoparticles. Chemical Engineering Journal, 180: 81-90.

[27] Dawodu, F. A, Akpomie G.K, and Ogbu, I (2012). The removal of cadmium (ii) ions from aqueous solution by the use of "afuze" bentonite: equilibrium, kinetic and thermodynamic studies. International Journal of Scientific and Engineering Research, 3(12): 1-8.

[28] Bayat, B. (2002). Comparative study of adsorption properties of Turkish fly ashes I. The case of nickel(II), copper(II) and zinc(II). Journal Hazardous Material, 95: 251–273.

[29] Ahmed, A. S., Tantawy, A. M., Abdallah, M. E and Qassim, I. M. (2015). Characterization and application of kaolinite clay as solid phase extractor for removal of copper ions from environmental water samples, International Journal of Advanced Research. 3(3): 1-21

[30] Riebe, B., and Bunnenberg, C (2007). "Influence of Temperature Pre-Treatment and High-Molar Saline Solutions on the Adsorption Capacity of Organo-Clay Minerals". Physics and Chemistry of the Earth Journal, 32: 581–587.

[31] Ajay K. A., Mahendra S. K., Chandrashekhar P. P., Ishwardas L. M., (2015). Kinetics study on the adsorption of ni2+ ions onto fly ash. Journal of Chemical Technology and Metallurgy, 50 (5): 601-605.

[32] Nanganoa, L.T. Ketcha, J.M. and Ndi, J.N. (2014). Kinetic and Equilibrium Modeling of the Adsorption of Amaranth from aqueous solution onto Smectite Clay. Research Journal of Chemical Sciences, 4(2): 7-14.

[33] Sodeinde K. O., Olusanya, S. O., Momodu, D. U., Enogheghase V. F., Lawal O. S (2021): Waste glass: An excellent adsorbent for crystal violet dye, Pb2+ and Cd2+ heavy metal ions decontamination from wastewater, Journal of the Nigerian Society of Physical Sciences, 3: 414–422

[34] Belhachemi M and Addoun F. (2011). Comparative adsorption isotherms and modeling of methylene blue onto activated carbons, Journal of applied Water Sciences, 1:111–117

[35] Muhammad B. I and Jimoh W.L.O (2012). Thermodynamics And Adsorption Isotherms for the Biosorption of Cr(vi), Ni(ii) and Cd(ii) onto Maize Cob, Chemsearch Journal 3(1): 7 – 12

[36] Bousba, S and Meniai H.A. (2013). Adsorption of 2-Chlorophenol onto Sewage Sludge based Adsorbent: Equilibrium and Kinetic Study. Chemical Engineering Transactiions, 35:859-864

[37] Tan, J., Zhang, X., Wei, X and Wang, L. (2012). Basic dye ssorption on ONP fiber. Bio-resources Journal, 7(3): 4307-4320

[38] Jameel, M. D., Hussien, A. K and Nasser, T. (2012). Removal of Cadmium Ions from Industrial Wastewater Using Iraqi Ceratophyllum Demersum. Al- Mustansiriyah Journal Science. 32(8): 71-84

[39] Dula, T., Siraj. K. and Kitte, S, A. (2014). Asdorption of hexavalent chromium from aqueous solution using chemically activated carbon prepared from locally available waste of bamboo. International scholarly Research Notices in Environmental chemistry, 2: 1-10.